BJR
© 2015 The Authors. Published by the British Institute of Radiology

Received: 15 June 2015 | Revised: 26 August 2015 | Accepted: 23 September 2015

doi: 10.1259/bjr.20150487

Cite this article as:
Jaspan ON, Fleysher R, Lipton ML. Compressed sensing MRI: a review of the clinical literature. *Br J Radiol* 2015; **88**: 20150487.

REVIEW ARTICLE

Compressed sensing MRI: a review of the clinical literature

[1]OREN N JASPAN, BS, [2]ROMAN FLEYSHER, PhD and [3]MICHAEL L LIPTON, MD, PhD

[1]Albert Einstein College of Medicine, The Bronx, NY, USA
[2]The Gruss Magnetic Resonance Research Center, Department of Radiology, Albert Einstein College of Medicine, The Bronx, NY, USA
[3]The Gruss Magnetic Resonance Research Center, Departments of Radiology, Psychiatry and Behavioral Sciences and The Dominick P. Purpura Department of Neuroscience, Albert Einstein College of Medicine, The Bronx, NY, USA

Address correspondence to: Dr Michael L Lipton
E-mail: *michael.lipton@einstein.yu.edu*

ABSTRACT

MRI is one of the most dynamic and safe imaging techniques available in the clinic today. However, MRI acquisitions tend to be slow, limiting patient throughput and limiting potential indications for use while driving up costs. Compressed sensing (CS) is a method for accelerating MRI acquisition by acquiring less data through undersampling of *k*-space. This has the potential to mitigate the time-intensiveness of MRI. The limited body of research evaluating the effects of CS on MR images has been mostly positive with regards to its potential as a clinical tool. Studies have successfully accelerated MRI with this technology, with varying degrees of success. However, more must be performed before its diagnostic efficacy and benefits are clear. Studies involving a greater number radiologists and images must be completed, rating CS based on its diagnostic efficacy. Also, standardized methods for determining optimal imaging parameters must be developed.

INTRODUCTION

MRI is one of the pre-eminent imaging modalities used in clinical practice today. Its ability to provide soft-tissue contrast is unmatched by most, if not all other imaging modalities. MRI can survey and quantify metabolic and physiological features of tissue, yielding valuable information about pathological processes that would otherwise be difficult to assess non-invasively. Not to be overlooked, MRI does not expose patients to dangerous ionizing radiation, making it safer than CT, the modality most likely to replace MRI, when MRI is not available or contraindicated. These properties of MRI contribute to its potential to be the most versatile imaging tool available to physicians.

However, a major obstacle to realizing this potential in many applications is limited imaging speed. MR images are thus susceptible to motion-related artefacts, which may even necessitate sedation or anaesthesia. Relatively low temporal resolution limits MRI of body parts that move with respiration, such as in abdominal[1] and cardiac imaging.[2] Long scan times increase costs and limit the number of patients for whom MRI is available.[3] For these reasons, physicians often seek alternate paths to diagnose patients and are routinely compelled to use CT instead of MRI, despite the added risk of exposure to ionizing radiation.[4]

The issue of long acquisition times in MRI stemming from segmented sampling of the *k*-space was recognized soon after its consideration as a clinical tool; attempts to accelerate MRI date to the late 1970s, before MRI was generally available for clinical use.[3] Motivations for increasing imaging speed included the limitations described above and especially the demands of physiological measurements that require higher spatial and/or spectral resolutions.[5] Because for a given sequence structure, the number of segments in *k*-space is a direct determinant of image acquisition time, methods for accelerating MRI commonly involve reducing their number, *i.e.* undersampling *k*-space. These approaches capitalize on the inherent redundancy in MR images, where individual points in *k*-space do not arise from distinct spatial locations.[6] Examples of this strategy include partial Fourier reconstruction[7] and parallel imaging (PI).[8,9] PI has made its way into the mainstream of clinical imaging. This approach exploits the fact that concurrently collected signals from coils with different spatial sensitivities carry distinct information about spatial localization complementing conventional spatial encoding and allowing skipping acquisition of *k*-space points.[10] However, PI acceleration factors >2 are not reliably achievable in the clinic, without unacceptable image degradation.[1]

Within the past decade, another technique has been developed and has been applied to accelerate MRI acquisition.

Compressed sensing (CS) is also founded on the premise of reconstructing an image from an incompletely filled *k*-space.[6,11,12] Unlike PI, however, in CS, no complementary information is collected. The inspiration for CS came from attempts to solve a somewhat related imaging problem: storage and transmission of increasingly large imaging data sets. The solution to this problem was lossy image compression, a process that reduces file size by permanently discarding certain data elements. Using a variety of algorithms, medical images can be successfully compressed while preserving diagnostic efficacy, even at compression ratios from 9 : 1 to 25 : 1.[13] Advances in image compression prompted Candes et al[11] and Donoho[12] to raise a series of questions which Lustig et al[6] summarized in the context of MRI: "Since the images we intend to acquire will be compressible, with most transform coefficients negligible or unimportant, is it really necessary to acquire all that data in the first place? Can we not simply measure the compressed information directly from a small number of measurements, and still reconstruct the same image, which would arise from the fully sampled set? Furthermore, since MRI measures Fourier coefficients …, the question is whether it is possible to do the above by measuring only a subset of *k*-space."

Affirmative answers to these questions form the basis of CS for accelerating MRI acquisition. Operationally, the reconstructed image must be consistent with the Fourier transform of the acquired *k*-space data and have few large-valued coefficients when sparsely transformed. Mathematically, this entails solving an optimization problem, *i.e.* finding the image that minimizes this form:[6]

$$\min_{x} \left(\|S - Fx\|_2^2 + \lambda \|\Psi x\|_1 \right) \qquad (1)$$

where x is the reconstructed image, S is the measured *k*-space data, F is Fourier transform, Ψ is a sparsifying transform and λ is a regularization parameter weighting relative importance of the two terms. The symbols $\|\ldots\|_1$ and $\|\ldots\|_2^2$ denote sums of absolute values and their squares, respectively.

Since 2007, the body of literature concerning CS and its application to a multitude of different clinical MR applications has increased at a near-exponential rate (Figure 1a). However, publications are largely focused on technical aspects of methodology and implementation; few studies[1,2,14–29] have examined the quality and diagnostic efficacy of accelerated CS images (Figure 1b). This review evaluates the literature assessing performance of CS for clinical applications, where diagnostic efficacy is of the utmost importance. Momentum for clinical use of CS continues to build, pushing this burgeoning technology towards the cusp of widespread clinical availability. It is imperative that clinical implementation be guided by an evidence base supporting its clinical validity and diagnostic utility. This review will thus identify the current evidence base and delineate remaining gaps in knowledge, to be addressed by future research.

METHODS

A structured literature search was conducted using the PubMed database to identify all pertinent articles published as of June 2014. The search terms used were as follows: "compressed sensing MRI" and "compressive sensing MRI". These searches yielded a total of 281 articles, 269 of which were unique. The references cited within these articles were probed for any additional relevant articles that were missed in the original searches. Of this contingent of articles, 18 articles[1,2,14–29] survived our exclusion criteria and were included in the review. Articles were excluded from the review if they met any of the following criteria: language other than English; study of CS and related technology in applications other than medical MRI; studies exclusively investigating CS as a method or technology rather than its implementation and efficacy in one or more specific clinical applications; animal studies; and reviews.

In order to facilitate a meaningful analysis of the different study designs used across the clinical CS research, we grouped methods based on their fundamental assessment of two overarching attributes: (1) image quality or (2) diagnostic efficacy. We define image quality as any assessment or scoring of an image based on its inherent characteristics and diagnostic efficacy as any assessment or measurement of an image's utility in

Figure 1. The number of articles per year (a) on the topic of compressed sensing MRI and (b) met the inclusion criteria for review in this article.

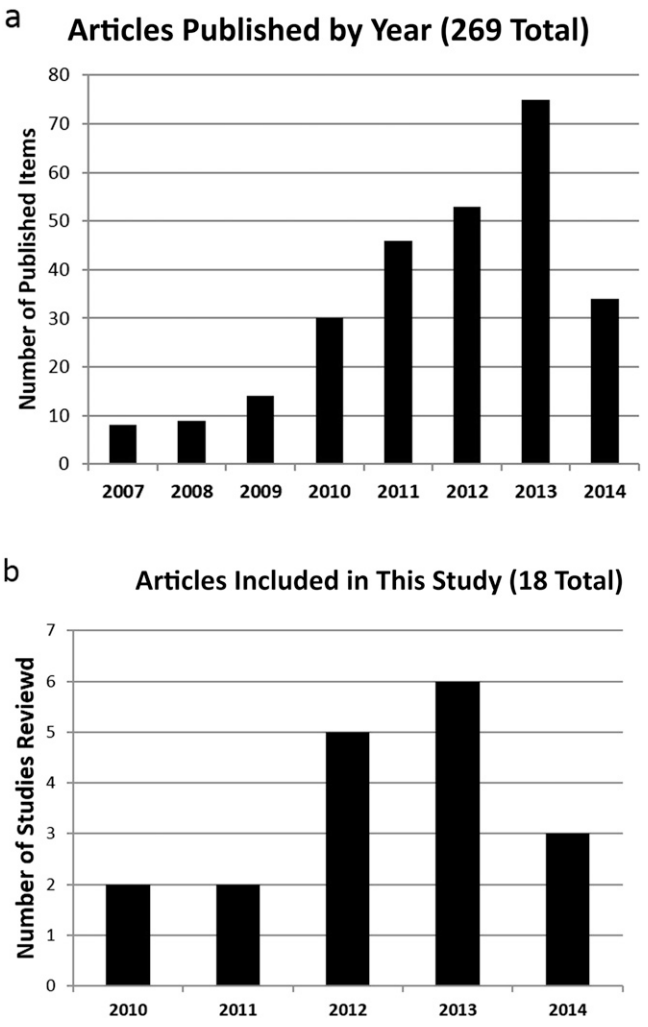

Figure 2. Scheme for categorizing the study design of each article. Studies were first grouped as to whether they evaluated image quality or diagnostic efficacy (some assessed both). These studies were then further classified as to whether they employed qualitative or quantitative assessment methods.

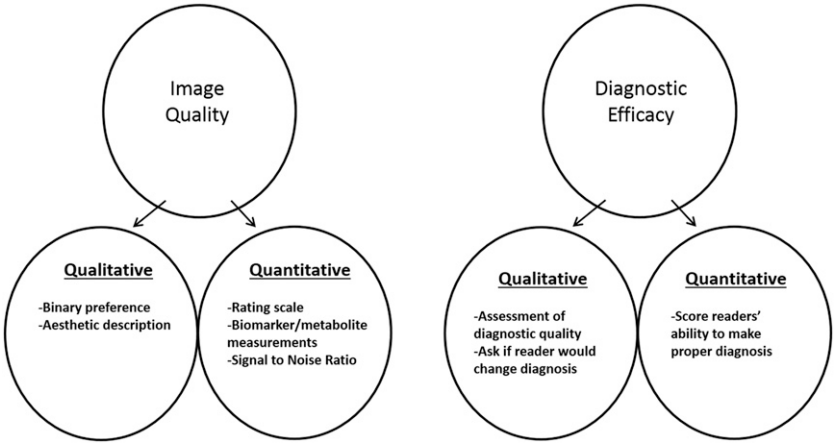

making an accurate diagnosis, in comparison with an external standard. Each of these two characteristics can be assessed qualitatively or quantitatively, as shown in Figure 2. All of the assessment criteria used by each of the studies is available in the Supplementary Table A.

RESULTS

Clinical applications of compressed sensing

Decades of research studying the effects of compression on different types of medical images has provided evidence that the "tolerance" of an image to compression is dependent on the modality and the nature of the anatomical and pathological content of the image.[30] Therefore, the degree of compression implemented in the clinical setting is dependent upon these same factors.[31] It stands to reason that CS, a technology related to image compression, should similarly be evaluated across the breadth of MRI applications and anatomical regions. The 18 articles included in this review evaluated the effect of CS on a wide range of MR applications (Figure 3). These studies assessed image quality at different acceleration rates and reported to what extent remained acceptable in the face of acceleration (Table 1).

Figure 3. The number of studies that have evaluated compressed sensing with each MR application: dynamic contrast-enhanced MRI (DCE-MRI);[14,16,28] paediatric MRI;[1,29] MR angiography;[15,27] MR spectroscopy of the brain and prostate[17] and for the measurement of phosphocreatine regeneration in muscle;[20] phase-contrast MRI for cardiac imaging[2,18] and vascular flow quantification;[24,25] sodium MRI for early detection of osteoarthritis;[19] chemical shift imaging for fat fraction quantification in Becker's muscular dystrophy;[22] multispectral imaging (MSI) of the spine;[26] contrast-enhanced multiphase MRI of the liver;[21] and brain MRI.[23] Subjects imaged in the paediatric MRI studies were referred for abdominal, cardiac, knee or cholangiopancreatography.

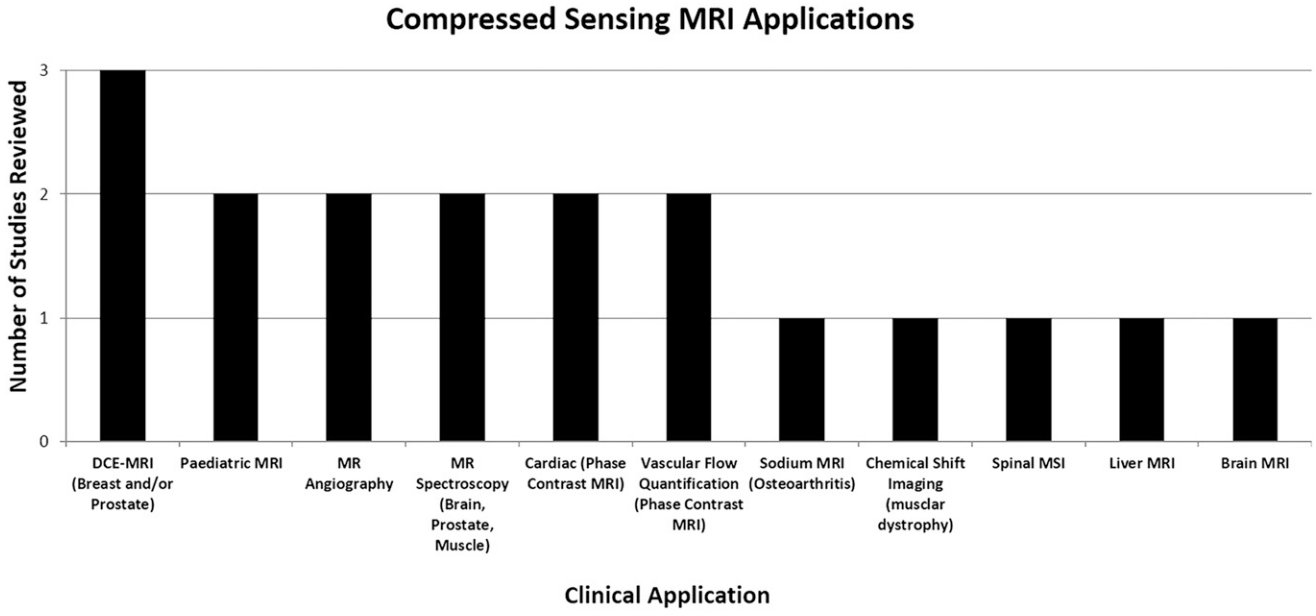

Table 1. Acceleration rates achieved and attempted for each compressed sensing (CS) MRI application studied

Compressed sensing MR application	Highest acceleration rate achieving "acceptable" image	Highest acceleration rate attempted
DCE-MRI (breast)[14,16]	10×,[14] 2×[16]	10×,[14] 4×[16]
DCE-MRI (prostate)[28]	2×	2×
Paediatric MRI[29]	7.2×	7.2×
MRA[27]	12.5×	12.5×
MRS (brain and prostate)[17]	5×	10×
Phosphorous MRS (muscle)[20]	2×	3×
Cardiac[2]	4.84×	4.84×
Vascular flow quantification[25]	4–5×	4–5×
Sodium MRI[19]	2×	4×
Chemical shift imaging[22]	4.94×	6.42×
Spinal MSI[26]	2×	2×
Liver MRI[21]	Not specified	Not specified
Brain MRI[23]	2×	4×

MRA, MR angiography; MRS, MR spectroscopy; MSI, multispectral imaging.

Study design

Although CS is a method for accelerating imaging by undersampling *k*-space at acquisition, it can also be "simulated" by undersampling a complete *k*-space, *i.e.* discarding part of the *k*-space data prior to the inverse Fourier transform, which creates the image. This latter approach is more convenient in the research setting because multiple permutations of undersampling can be tested, without additional scan time. Additionally, all undersampled images can be compared with the fully sampled conventional reference image from which they were derived. Many researchers refer to this "simulation" of CS as retrospective CS or retrospective CS reconstruction.[15–17,20,23,26,27] Standard undersampling of *k*-space at acquisition is often referred to as prospective CS or prospective undersampling to distinguish the two methods. Both prospective and retrospective study designs for CS image acquisition were observed among the 18 articles reviewed (Figure 4). 15 studies used only one of the 2 designs: 9 studies performed only prospective CS[1,2,18,21,22,24,25,28,29] and 6 studies performed only retrospective CS.[14–17,19,23] Three studies used both prospective and retrospective CS.[20,26,27] In all three of these cases, CS was retrospectively simulated prior to the performance of prospective CS acquisitions. The rationale for performing both retrospective and prospective CS in the same study were: (1) to validate the CS technique;[20] (2) to confirm that prospective undersampling did not affect the image quality results;[26] and (3) to select a reconstruction algorithm prior to implementing it in a prospective study.[27] No advantage in the achievable acceleration was discernable between studies using prospective or retrospective CS.

A total of 1306 sets of images were generated from the 275 subjects across the 18 articles. We define a "set" of images as the images acquired from a patient using a given acquisition method, reconstruction algorithm and acceleration rate. All 18 articles explained their methodology for creating these image sets. Each study generated several image sets, which they then compared to evaluate the quality of the images or diagnostic efficacy at one or more acceleration rate. A full breakdown of the image sets described by each study is included as Supplementary Table A.

Study subjects and image evaluators

Sample size and makeup is an important consideration when evaluating new imaging techniques, as is the number and state of blinding of the image evaluators.[32] A total of 275 subjects were imaged across the 18 studies (range, 3–34; mean = 15.28; median = 11.5; standard deviation = 10.23). 7 studies imaged healthy subjects,[15,19–21,23,24,27] and 11 imaged patients referred for the type of imaging under consideration[1,2,14,16–18,22,25,26,28,29] (Figure 5).

Images were either evaluated by human readers or scored based on quantitative criteria. In the studies reviewed, there were 19 total human readers, 17 of whom were radiologists. Of these 17 radiologists, 8 were explicitly characterized as "board certified". The other 9 radiologists were described as "experienced" in evaluating the types of images in their given studies. This experience ranged from 1 to 20 years. The two non-radiologist human readers were an MR physicist and a senior research radiographer, each with 7 years of experience with muscle imaging, the area of focus in this study.[22] In 10 studies human readers rated images.[1,15,18,21–23,26–29] In eight studies, accurate measurement of a quantitative metric with CS MRI (*e.g.* contrast uptake or metabolite concentration) was assessed.[2,14,16,17,19,20,24,25] The breakdown of the number of image evaluators included across studies and the degree to which they were blinded to patient or image information is presented in Figures 6 and 7, respectively.

Figure 4. The number of studies that performed prospective compressed sensing acquisition, retrospective compressed sensing simulation on fully sampled data sets and both methods.

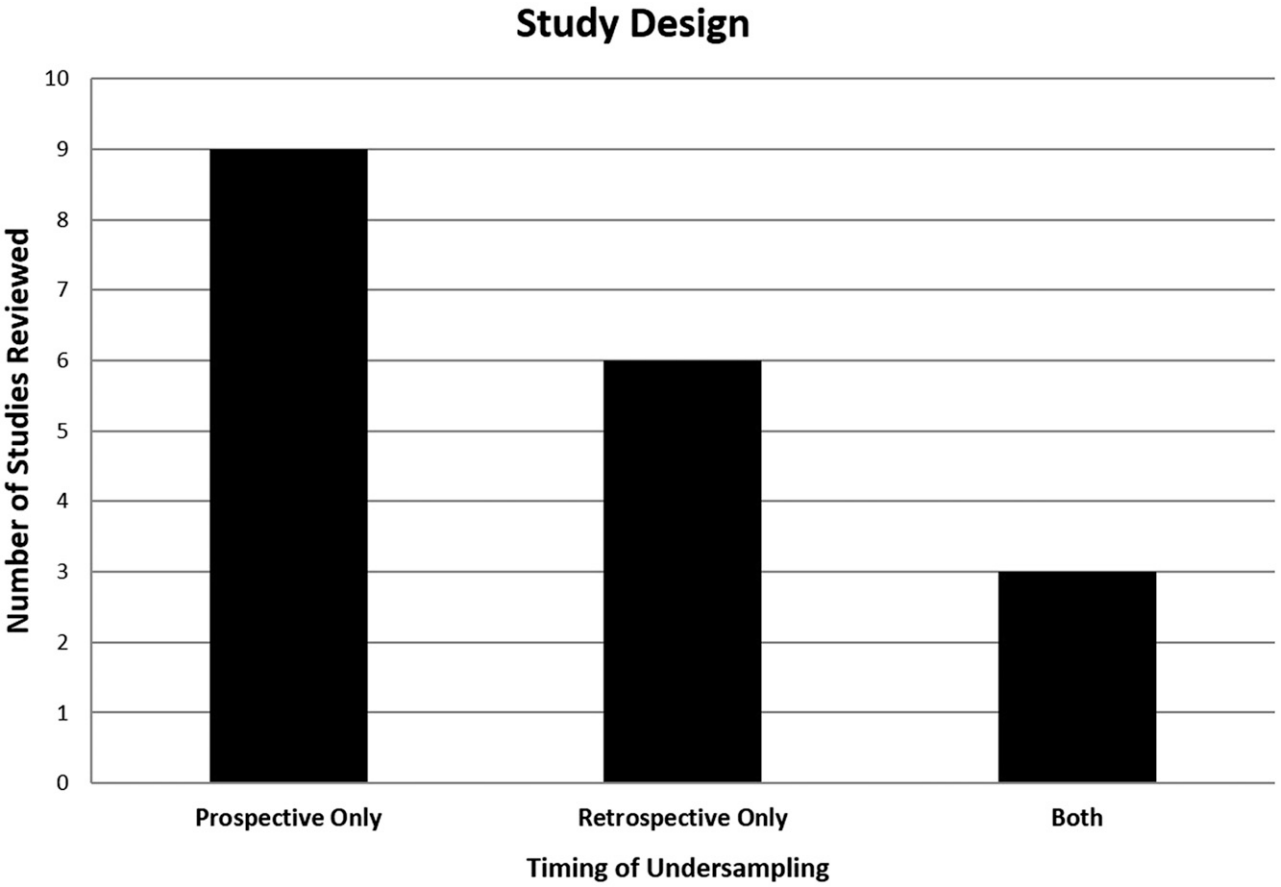

Imaging acceleration

A wide range of acceleration factors was tested across the 18 studies. Since CS accelerates image acquisition by undersampling *k*-space, it follows that the average density of *k*-space sampling is inversely proportional to acceleration. For example, an acquisition that randomly samples only 25% of *k*-space would be accelerated by a factor of 4 relative to the same acquisition where all points in *k*-space are sampled. Such undersampling is achieved by a four-fold reduction of number of acquired *k*-space lines in Cartesian sampling; number of projections or spirals in radial or spiral sampling and number of *k*-space points in chemical shift imaging. This is because each type of *k*-space sampling has one dimension along which sampling is "free": a line, a spoke, a spiral and time respectively.

Fully sampled images were often used as the gold-standard reference, and were either acquired, or already existed in the case of the retrospective CS reconstructions. Acceleration factors up to 12.5× were tested, achieving varying degrees of success in producing images insignificantly different from standard imaging techniques or of acceptable diagnostic efficacy relative to the standard images (Figure 8). All but four studies acquired or used fully sampled images as controls.[1,25,27,29] Reasons for not employing this standard included: studies (1) aimed to test the effects of CS + PI relative to PI alone,[1,29] (2) relied upon conservation of blood flow as an internal physiologic control,[25] or (3) partial Fourier reconstruction accelerated 1.6× served as a gold standard.[27]

All eight studies that tested acceleration factors up to 2× reported diagnostically acceptable images or images not significantly different from gold standard images at a given degree of undersampling.[15–17,19,20,23,26,28] In only two of these studies was acceleration also successfully pushed beyond 2×.[15,17] Of the 27 tests of acceleration factors >2, 18 tests were successful while 9 failed to produce acceptable images. The highest degree of acceleration that yielded acceptable images was 12.5×, for contrast-enhanced MR angiography.[27] Results of all acceleration factors tested in each study is included as Supplementary Table A.

Combined compressed sensing and parallel imaging

Eight studies combined CS with PI in order to multiply their maximum acceleration.[1,2,18,21,22,25,28,29] All of these studies found that the combined methodology produced images deemed acceptable or not significantly different from fully sampled images, while employing acceleration rates from 2× to 7.2×, depending on the application. Five of these studies compared the combined method with the standard imaging protocol for the respective study's imaging application.[2,18,21,22,28] One study used conservation of blood flow to the upper, lower and whole body as an internal control.[25] The other two studies compared the images acquired by PI alone with those acquired

Figure 5. The breakdown of imaging subjects across studies, grouped as healthy subjects and patients.

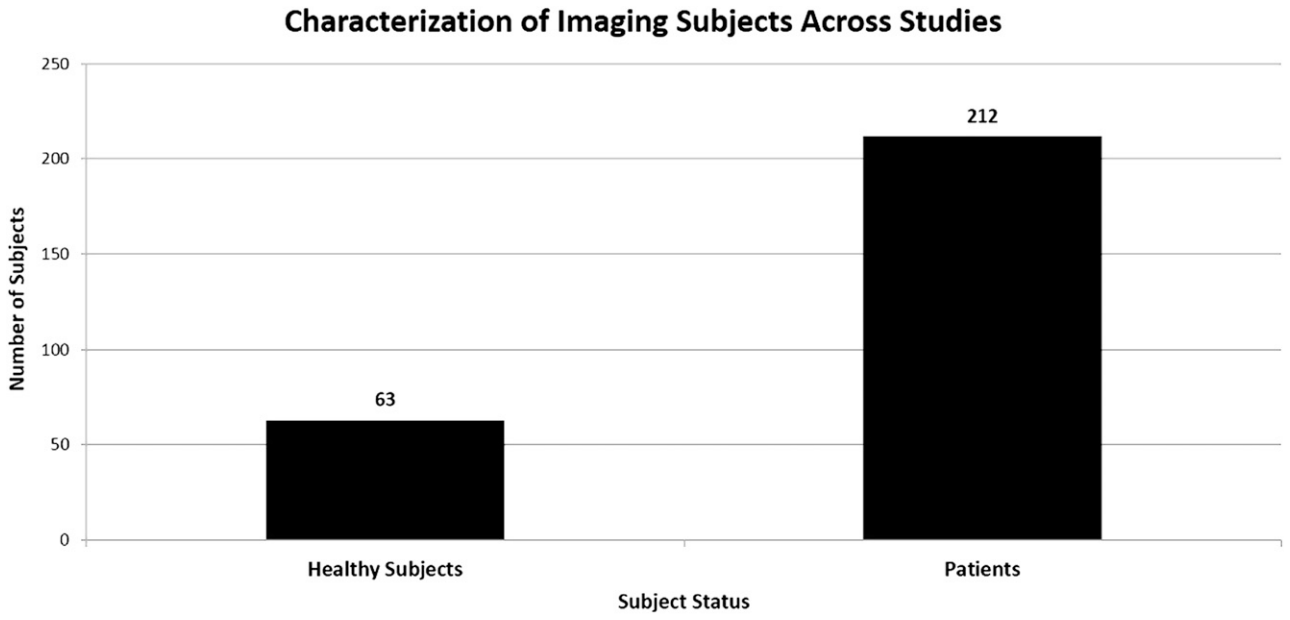

with the combined CS + PI method.[1,29] In all eight of these studies, the authors concluded that combining CS and PI results in better images than when PI is implemented on its own. The combination of CS and PI did not systematically increase the acceleration rates, yielding acceptable images in comparison with CS implemented on its own. Across all attempts to exceed an acceleration factor of 2×, six approaches (across five studies) were successful with combined CS + PI.[1,18,22,25,29]

Sparsifying transform and reconstruction

In addition to the data that are collected, CS image reconstruction depends on three additional factors, expressed in Equation (1): (a) the *k*-space undersampling strategy, (b) the sparsifying transform and (c) the value of the regularization parameter. The different parameter choices made by the authors of the reviewed studies are summarized in Table 2. Nine of the studies[15–20,22,23,27] either reported the parameters explicitly or

Figure 6. The number of studies which utilized a given number of human evaluators to evaluate the images. Studies which did not utilize human image evaluators assessed images by measuring certain image attributes. Nine of the studies included two evaluators,[1,15,18,21–23,27–29] and one study included one evaluator.[26]

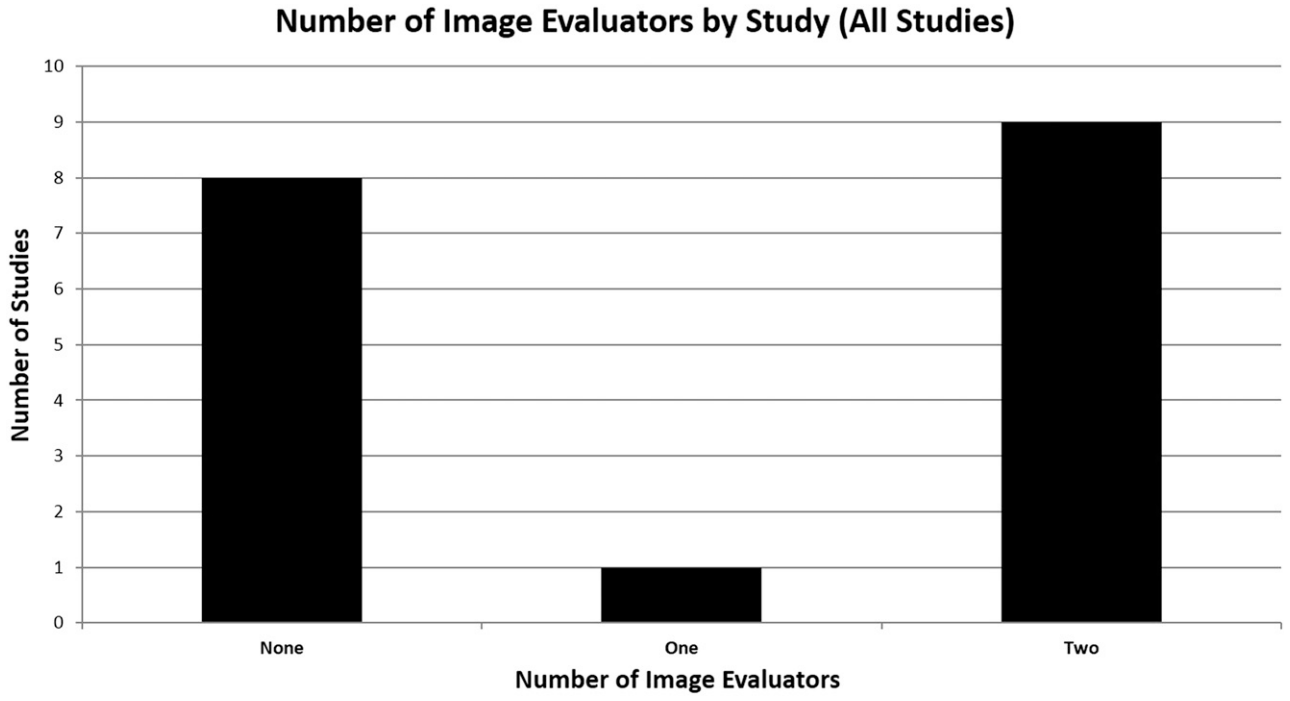

Figure 7. The number of image evaluators across studies who were blinded to image type or patient history or not blinded to this information. Of the 19 radiologists, 15 were blinded to image type, patient history or both. Four radiologists across two studies were not blinded with regard to image type or patient history.[1,28]

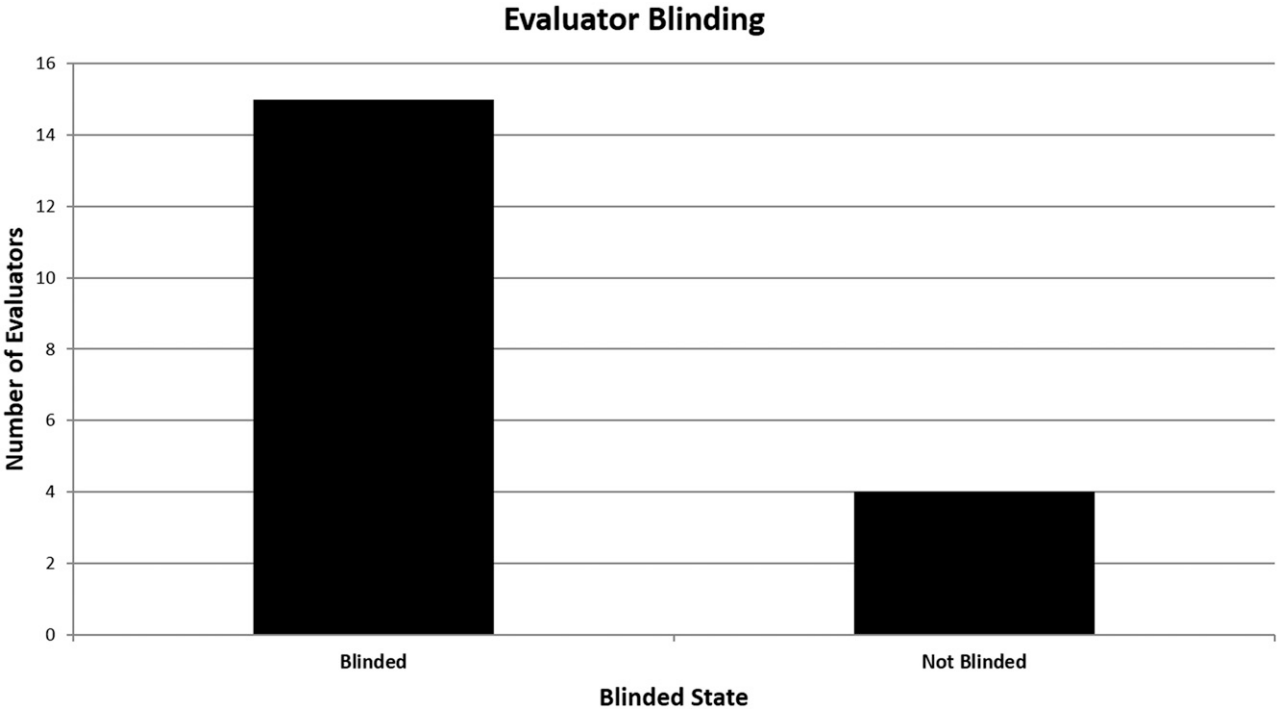

cited correspondingly in Greengard et al,[33] Lustig and Pauly,[34] Feng et al,[35] Uecker et al,[36] Zhang et al[37] where each could be found, though the available information may have been incomplete. Simply describing the sparsifying transform as a wavelet type, for example, still leaves many details unclear as there are many types of wavelets, each with different properties.[38] All of the studies utilized undersampling strategies, which either fully sampled the centre of *k*-space or sampled it more densely than the periphery of *k*-space. When Poisson disc or Gaussian sampling was used, the parameters of these distributions (minimum distance between points and its dependence on location in *k*-space for Poisson-disc sampling or width of the Gaussian sampling) were not always specified. While intuitive or semianalytic substantiation of the choice of sparsifying transform and sampling strategy can be found, the greatest challenge is presented by the regularization parameter. As seen in Table 2, the regularization parameter appears to depend on image type, acceleration factor, sparsifying transform, sampling scheme etc. Importantly, it also depends on how the data are scaled. Indeed, Equation (1) verifies that scaling the measured data S and the reconstructed image x by a factor of 2 also requires corresponding scaling of the regularization parameter. Thus, for the value of the regularization parameter to convey useful information, the scaling of the data needs to be described. Only one study, by Akcakaya et al,[15] reported how the data were scaled. All studies noted that the value of the regularization parameter impacts perceived image quality, artefacts or synthetic appearance.

Another relevant aspect of image reconstruction is its speed. Given non-linear and iterative nature of the available algorithms, the reconstruction is inherently slow. Tabulating their performance requires standardization of the task: type of acquisition, *k*-space undersampling strategy, sparsifying transform etc. and therefore is more appropriate for a technical review of CS. Nevertheless, long delay between image acquisition and its availability for review by a radiologist presents a barrier for the widespread clinical use of CS. Depending on the task and algorithm, the delay may be between 30 and 210 min.[1,14,19] However, we remain optimistic that through a combination of increased central processing unit speeds, parallel computing, graphics processing unit implementation and maturation of algorithms, this impediment will be resolved over time.

Image assessment

The 18 articles varied substantially in their methods for evaluating images. Figure 9 presents the breakdown of the number of studies whose assessment methods fit each of the above classifications. 8 of the 16 quantitative assessments of image quality used radiologists as readers.[15,21–23,26–29] Each reader rated images on a numerical scale, based on the delineation or clarity of a given set of anatomical landmarks or lesion borders, in addition to other criteria. The other eight articles that quantitatively evaluated image quality rated a CS image by comparing it to a measurement made with standard imaging. These comparisons included correlation between contrast uptake curves;[14] voxel intensities;[16] metabolite maps and intensities;[17] ventricular volume, ejection fraction and various vascular flow rates;[2] signal-to-noise ratio (SNR) and tissue sodium concentration;[19] muscle phosphocreatine resynthesis rate;[20] and various vascular velocity and flow rates.[24,25] In the only article that qualitatively assessed image quality, Vasanawala et al[1]

Figure 8. Acceleration rates tested across studies. Grey indicates the number of studies that obtained images deemed acceptable at a given acceleration rate, and black indicates the number of studies that obtained unacceptable images.

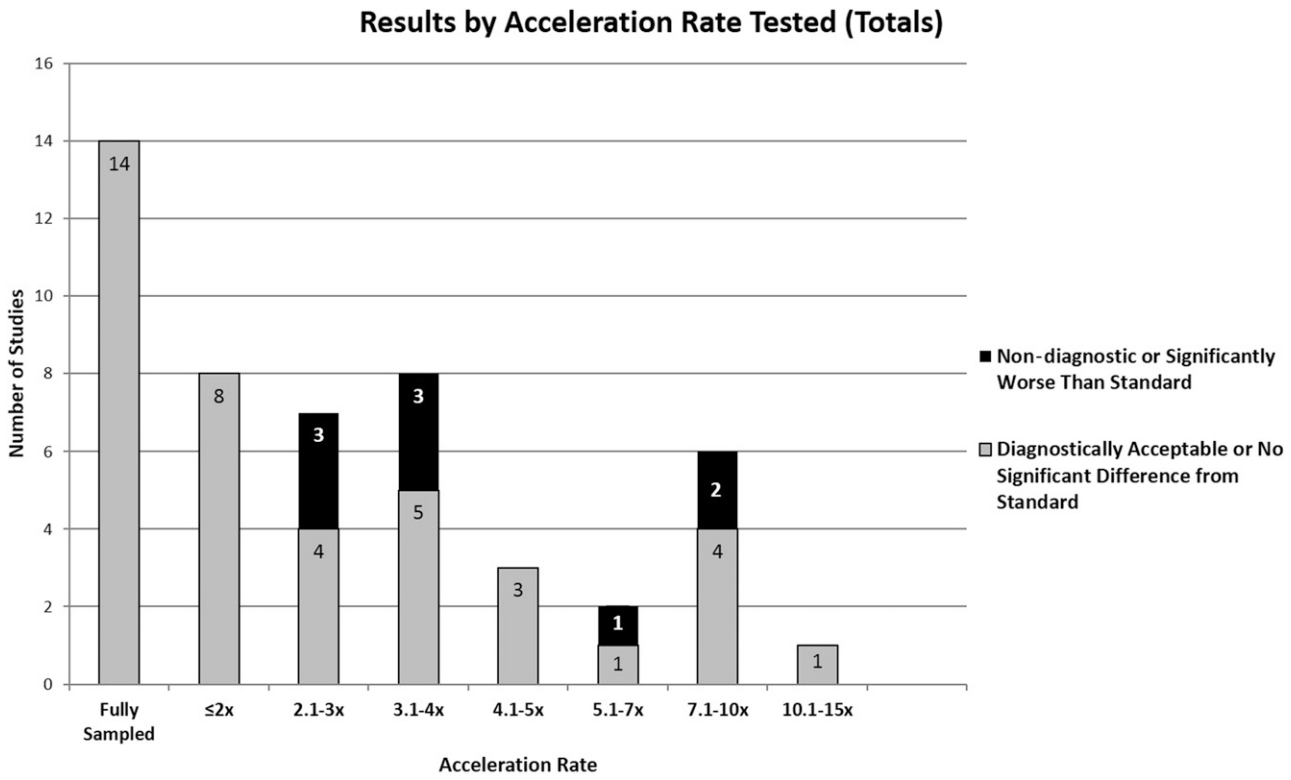

asked radiologists to rate images as "good quality", "limited" or "non-diagnostic", to indicate their preference for images acquired *via* combined CS and PI or PI alone and to compare anatomical structure delineation between the two accelerated imaging methods.

Only three articles specifically assessed the diagnostic efficacy of CS MRI. In these studies, CS imaging was used to attempt diagnosis of brain lesions,[23] abdominal lesions[29] and either cardiac valvular insufficiency or extracardiac shunts.[18] The qualitative assessments of diagnostic efficacy either asked radiologists to judge the clinical diagnostic quality of the reconstructed images[23] or to select an image quality score threshold for diagnostic utility.[29] Hsiao et al[18] authored the only quantitative assessment of the diagnostic efficacy of CS MRI. In this study of cardiac imaging, two radiologists blinded to patient history were asked to note the presence of valvular regurgitation at any valve and to tabulate the presence of any intracardiac or extracardiac shunts. Their ability to accurately diagnose these pathologies using CS MRI, standard MRI and echocardiogram was compared. Echocardiogram was considered the gold standard for detecting these lesions. Intermodality agreement between CS MRI and echocardiogram was calculated for each of the two radiologists (AH and SSV). Sensitivity and specificity of CS MRI were also calculated with respect to echocardiography as the gold standard. Based on these measures, the authors concluded that the radiologists were able to reliably diagnose valvular insufficiency and extracardiac shunts with CS MRI.

Compressed sensing artefacts

Image artefacts affect perception and disrupt readers to varying degrees.[39] Sharma et al[23] (brain MRI), Worters et al[26] (spine MSI) and Zhang et al[29] (paediatric abdominal MRI) were the only studies we reviewed that systematically described artefacts observed in CS. In the study of brain MRI, artefacts became prominent and disruptive to diagnosis at acceleration factors $>2\times$. The two primary artefacts observed in this study were "global ringing" and blurring of fine detail. The authors concluded that these artefacts would hinder the accurate diagnosis of pathology but suggested that $2\times$-accelerated data acquisition might be possible for sequences with higher native spatial resolution. Worters et al[26] described "slight blurring" of CS reconstructed images, which they suggested was due to the denoising effect of CS reconstruction. Up to 17% of CS abdominal images were judged to have significant blurring, which rendered them non-diagnostic.

DISCUSSION

All 18 studies we reviewed were generally enthusiastic regarding the potential of CS as a clinical tool. However, there remain important gaps in knowledge that should be addressed before CS is transitioned to routine clinical use. Only this small body of literature addresses the effects of CS on medical images, of which only a small subset examined the actual clinical diagnostic efficacy of CS MRI.

US Food and Drug Administration (FDA) guidelines for empirical evaluation of new imaging technology[32] include three

Table 2. Compressed sensing parameters

Study	Sparsifying transform	Undersampling strategy	Regularization
Vasanawala et al[1]	Wavelet	Poisson disc	
Wang et al[14]	Spatial finite difference or discrete wavelet transformation	Undersampling in both *ky* and *kz* phase-encoding directions using a 2D Gaussian random distribution	
Akcakaya et al[15]	Sparsity in terms of the number of non-zero intensity voxels	The central *k*-space region is densely sampled in diamond-like shape with 24-point diagonal. The edges of the *k*-space were sampled using a zero-mean Gaussian-probability density	The regularization parameter was set to 2/500 of the maximum of the zero-filled image for the first 50 iterations and 2/100 of the maximum for the last 10 iterations
Smith et al[16]	Magnitude of image intensity gradient	The central *k*-space region is fully sampled. At higher frequencies the sampling density of phase encodes follows k^{-1}, where *k* is spatial frequency	$\lambda = 0.1$
Geethanath et al[17]	Daubechies wavelet transform and total variation	The central *k*-space region is fully sampled in 2D. The extent of the fully sampled centre was dependent on the inverse of the acceleration factor. At higher *k*, the sampling density of phase encodes follows k^{-n}, n is not specified	Experimentally determined $\lambda_w = 0.001$ and $\lambda_{TV} = 0.005$
Hsiao et al[2]		Poisson disc	
Hsiao et al[18]	Wavelet transform	Variable density Poisson-disc *k*-space undersampling in phase encode (2D slices)	$\lambda = 0.015$
Madelin et al[19]	Discrete cosine transform and total variation	The 3D radial acquisition with the spherical co-ordinates of the spokes chosen following the Rakhmanov–Saff–Zhou algorithm	$\lambda_w = 0.0005$, 0.0010, 0.0025, 0.0050, 0.0075, 0.0100 and $\lambda_{TV} = 0$, 0.0005, 0.0010, 0.0025, 0.0050, 0.0075, 0.0100
Parasoglou et al[20]	PCA—principal components in time domain	The sampling density of phase encodes follows k^{-3} in *ky*–*kz* phase encodes	$\lambda_{pca} = 0.01$
Chandarana et al[21]	Total variation in space and time	Golden-angle scheme of 2D radial acquisition	
Hollingsworth et al[22]	Daubechies 4 wavelet	Variable density Poisson-disc undersampling in *ky*–*kz*, with 24 × 24 fully sampled centre with quadratic fall in density from the *k*-space centre	$\lambda = 0.1$ determined by best match between CS reconstruction and reconstruction of the fully sampled data using RMSE and the SSIM
Sharma et al[23]	Daubechies 4 wavelet	Fully sampled centre of 10% *i.e.* 25 lines. Two sampling densities were evaluated k^{-2} and k^{-6} with the latter giving better performance	$\lambda = 0.002$ for 2×, 3×, 4× accelerations of T2-SE and 2× acceleration of T2-FLAIR; $\lambda = 0.001$ for T2-FLAIR at 3× and 4× accelerations
Tao et al[24]	Fourier	Full sampling of the central 20 rows of *k*-*t* space and the remaining *k*-*t* space being sampled with a uniform density, randomised pattern	
Tariq et al[25]		*k*-space data were acquired with variable density Poisson-disc undersampling in two-phase-encoding directions	
Worters et al[26]	Daubechies 4, in y–z	Gaussian-weighted variable density random sampling pattern	
Rapacchi et al[27]	Total variation	Three schemes: a uniform distribution, a Gaussian-probability density distribution and a Poisson-disc distribution where disc radius increases with distance to the centre of *k*-space. For all sampling patterns, 10% of the samples were distributed in the centre of *k*-space to acquire fully low frequency points	Determined by best match between CS reconstruction and reconstruction of the fully sampled data using RMSE excluding voxels in the lower 10% of the intensity scale to a void background noise
Rosenkrantz et al[28]	Total variation in space and time	Golden-angle ordering of radial acquisitions	
Zhang et al[29]	Wavelet	Variable density Poisson-disc *k*-space sampling	

2D, two-dimensional; 3D, three-dimensional; CS, compressed sensing; FLAIR, fluid-attenuated inversion recover; PCA, principal component analysis; RMSE, root mean square error; SE, spin echo; SSIM, structural similarity index.

Figure 9. Visual quantification of the image assessment methods implemented across the studies. Studies were divided based on the assessment of image quality or diagnostic efficacy and further classified based on quantitative or qualitative methodology. 17 articles assessed image quality, 16 quantitatively[2,14–17,19–29] and 1 qualitatively.[1] Three articles assessed the diagnostic efficacy of compressed sensing MRI, two qualitatively[23,29] and one quantitatively.[18] Note that some studies fall under multiple categories.

phases of trials through which new techniques should be evaluated: (1) exploratory/pilot (2) challenge/lab-based and (3) advanced clinical use. Based upon FDA criteria for the number of image readers and patient sample size, all of the existing literature on clinical use of CS is exploratory (1–3 image readers, 10–50 patients). FDA guidelines suggest that larger, multicentre trials of diagnostic efficacy, involving as many as 10 or more radiologists, should be completed. Given the ability to retrospectively undersample the existing medical images to simulate CS, no new images need be acquired to perform a large-scale study, which would therefore be financially and logistically feasible. However, merely increasing study size fails to address certain context-dependent obstacles, as described in the following paragraphs.

Some of the clinical CS studies reviewed here explicitly acknowledge limitations of the research that has been completed to this point. They articulate challenges that need to be overcome prior to routine clinical use and make suggestions for future research. The challenge most often noted by researchers is the difficulty of selecting parameters to optimize performance of CS.[2,22,23] In the cases where this challenge has been addressed, pilot studies or multiple iterations of image reconstruction were necessary to select parameters such as the sampling pattern, regularization parameter and sparsifying transform in order to optimize results. These articles acknowledged that such a trial-and-error approach would not be possible in a clinical setting. However, since the optimal values for some parameters may be a function of the compressibility of an image, a property which varies for different anatomical areas,[22] context-dependent optimization may prove essential. Sharma et al[23] suggest that a standardized method for selecting these parameters must be developed before CS can be routinely implemented in clinical protocols.

Further lessons may be learnt from the research on medical image compression. The degree to which images can be successfully compressed before they no longer retain acceptable quality for diagnostic use has been referred to as compression tolerance, which is thought to be influenced by several factors such as energy distribution between low and high spectral subbands,[30] SNR, the type of image contrast, pixel size and the specific organ or pathology being evaluated.[40] In other words, the tolerance of an image to compression is based on the type of image and the subject of the image. While it has been demonstrated that subjective losses in image quality can occur before the diagnostic efficacy of an image is lost,[41] the degree to which this is true must be established for a wide range of different types of images and pathology. It is vital that radiologists understand this context sensitivity and the potential consequences of CS reconstruction on the delineation of anatomy and detection of pathology, which may impact diagnostic performance.[23]

Research on imaging acceleration *via* PI highlights another potential gap in knowledge regarding CS: the effect of acceleration on SNR. It is known that SNR is proportional to voxel volume and to the square root of acquisition time.[42] In the case of PI, an excess of SNR degradation is observed with increasing acceleration factors. This excess degradation is characterized by a geometry factor, also known as the *g*-factor.[43] It is possible that a similar SNR-degrading factor also exists in CS MRI, a topic that warrants attention. However, SNR comparisons are only

valid when voxel dimensions are fixed. Unlike PI or conventional Cartesian imaging where voxel size is given by the ratio of field of view to number of phase-encode lines (adjusted for parallel acceleration factor), this definition does not apply in CS, as is evident by the blurring artefact seen in CS images, as discussed in the section entitled "Compressed sensing artefacts". Moreover, SNR is a function of the regularization parameter and can be made arbitrarily high: Equation (1) verifies that increase of regularization reduces the consistency of the reconstructed image with the noisy data leading to the reduction of noise in the image. Such trade of accuracy of image reconstruction for SNR *via* regularization has been explored in the context of PI;[44,45] however, it is not essential to the PI method. Therefore, nonlinear and denoising properties of CS reconstruction, which may also remove important diagnostic information, present a challenge for SNR characterization. A more promising approach is a recently developed framework for task-based assessment of image quality in CS which models clinical uses of MRI, such as identification and localization of abnormalities.[46]

The potential for CS to accelerate MRI acquisition with minimal effects on image quality is an exciting development for the future of radiology, and medicine as a whole. In this day of increased cognizance of healthcare costs, it is apparent that efficiency of all medical services is at a premium. This is especially true in MRI, a relatively costly and time-intensive imaging modality. Long acquisition times also limit the number of patients for whom the service is available and decrease the utility of MRI for many applications requiring high imaging speed. Thus, optimizing CS for various clinical MRI contexts is an important goal with potential to transform diagnostic imaging with respect to efficiency, cost-effectiveness and ultimately clinical utility.

REFERENCES

1. Vasanawala SS, Alley MT, Hargreaves BA, Barth RA, Pauly JM, Lustig M. Improved pediatric MR imaging with compressed sensing. *Radiology* 2010; **256**: 607–16. doi: 10.1148/radiol.10091218
2. Hsiao A, Lustig M, Alley MT, Murphy M, Chan FP, Herfkens RJ, et al. Rapid pediatric cardiac assessment of flow and ventricular volume with compressed sensing parallel imaging volumetric cine phase-contrast MRI. *AJR Am J Roentgenol* 2012; **198**: W250–9.
3. Cohen MS, Weisskoff RM. Ultra-fast imaging. *Magn Reson Imaging* 1991; **9**: 1–37.
4. Olsen OE. Imaging of abdominal tumours: CT or MRI? *Pediatr Radiol* 2008; **38**(Suppl 3): S452–8. doi: 10.1007/s00247-008-0846-5
5. Geethanath S, Reddy R, Konar AS, Imam S, Sundaresan R, D R RB, et al. Compressed sensing MRI: a review. *Crit Rev Biomed Eng* 2013; **41**: 183–204.
6. Lustig M, Donoho D, Pauly JM. Sparse MRI: the application of compressed sensing for rapid MR imaging. *Magn Reson Med* 2007; **58**: 1182–95. doi: 10.1002/mrm.21391
7. McGibney G, Smith MR, Nichols ST, Crawley A. Quantitative evaluation of several partial Fourier reconstruction algorithms used in MRI. *Magn Reson Med* 1993; **30**: 51–9. doi: 10.1002/mrm.1910300109
8. Pruessmann KP, Weiger M, Scheidegger MB, Boesiger P. SENSE: sensitivity encoding for fast MRI. *Magn Reson Med* 1999; **42**: 952–62.
9. Sodickson DK, Manning WJ. Simultaneous acquisition of spatial harmonics (SMASH): fast imaging with radiofrequency coil arrays. *Magn Reson Med* 1997; **38**: 591–603. doi: 10.1002/mrm.1910380414
10. Hutchinson M, Raff U. Fast MRI data acquisition using multiple detectors. *Magn Reson Med* 1988; **6**: 87–91.
11. Candes EJ, Romberg J, Tao T. Robust uncertainty principles: exact signal reconstruction from highly incomplete frequency information. *IEEE Trans Inf Theory* 2006; **52**: 489–509.
12. Donoho DL. Compressed sensing. *IEEE Trans Inf Theory* 2006; **52**: 1289–306. doi: 10.1109/TIT.2006.871582
13. Koff DA, Shulman H. An overview of digital compression of medical images: can we use lossy image compression in radiology? *Can Assoc Radiol J* 2006; **57**: 211–17.
14. Wang H, Miao Y, Zhou K, Yu Y, Bao S, He Q, et al. Feasibility of high temporal resolution breast DCE-MRI using compressed sensing theory. *Med Phys* 2010; **37**: 4971–81. doi: 10.1118/1.3483094
15. Akcakaya M, Hu P, Chuang ML, Hauser TH, Ngo LH, Manning WJ, et al. Accelerated noncontrast-enhanced pulmonary vein MRA with distributed compressed sensing. *J Magn Reson Imaging* 2011; **33**: 1248–55.
16. Smith DS, Welch EB, Li X, Arlinghaus LR, Loveless ME, Koyama T, et al. Quantitative effects of using compressed sensing in dynamic contrast enhanced MRI. *Phys Med Biol* 2011; **56**: 4933–46. doi: 10.1088/0031-9155/56/15/018
17. Geethanath S, Baek HM, Ganji SK, Ding Y, Maher EA, Sims RD, et al. Compressive sensing could accelerate 1H MR metabolic imaging in the clinic. *Radiology* 2012; **262**: 985–94. doi: 10.1148/radiol.11111098
18. Hsiao A, Lustig M, Alley MT, Murphy MJ, Vasanawala SS. Evaluation of valvular insufficiency and shunts with parallel-imaging compressed-sensing 4D phase-contrast MR imaging with stereoscopic 3D velocity-fusion volume-rendered visualization. *Radiology* 2012; **265**: 87–95. doi: 10.1148/radiol.12120055
19. Madelin G, Chang G, Otazo R, Jerschow A, Regatte RR. Compressed sensing sodium MRI of cartilage at 7T: preliminary study. *J Magn Reson* 2012; **214**: 360–5. doi: 10.1016/j.jmr.2011.12.005
20. Parasoglou P, Feng L, Xia D, Otazo R, Regatte RR. Rapid 3D-imaging of phosphocreatine recovery kinetics in the human lower leg muscles with compressed sensing. *Magn Reson Med* 2012; **68**: 1738–46. doi: 10.1002/mrm.24484
21. Chandarana H, Feng L, Block TK, Rosenkrantz AB, Lim RP, Babb JS, et al. Free-breathing contrast-enhanced multiphase MRI of the liver using a combination of compressed sensing, parallel imaging, and golden-angle radial sampling. *Invest Radiol* 2013; **48**: 10–16. doi: 10.1097/RLI.0b013e318271869c
22. Hollingsworth KG, Higgins DM, McCallum M, Ward L, Coombs A, Straub V. Investigating the quantitative fidelity of prospectively undersampled chemical shift imaging in muscular dystrophy with compressed sensing and parallel imaging reconstruction. *Magn Reson Med* 2013; **72**: 1610–19. doi: 10.1002/mrm.25077.
23. Sharma SD, Fong CL, Tzung BS, Law M, Nayak KS. Clinical image quality assessment of accelerated magnetic resonance neuroimaging using compressed sensing. *Invest Radiol* 2013; **48**: 638–45. doi: 10.1097/RLI.0b013e31828a012d
24. Tao Y, Rilling G, Davies M, Marshall I. Carotid blood flow measurement accelerated by compressed sensing: validation in healthy volunteers. *Magn Reson Imaging* 2013; **31**: 1485–91. doi: 10.1016/j.mri.2013.05.009

25. Tariq U, Hsiao A, Alley M, Zhang T, Lustig M, Vasanawala SS. Venous and arterial flow quantification are equally accurate and precise with parallel imaging compressed sensing 4D phase contrast MRI. *J Magn Reson Imaging* 2013; **37**: 1419–26. doi: 10.1002/jmri.23936
26. Worters PW, Sung K, Stevens KJ, Koch KM, Hargreaves BA. Compressed-sensing multispectral imaging of the postoperative spine. *J Magn Reson Imaging* 2013; **37**: 243–8. doi: 10.1002/jmri.23750
27. Rapacchi S, Han F, Natsuaki Y, Kroeker R, Plotnik A, Lehrman E, et al. High spatial and temporal resolution dynamic contrast-enhanced magnetic resonance angiography using compressed sensing with magnitude image subtraction. *Magn Reson Med* 2014; **71**: 1771–83. doi: 10.1002/mrm.24842
28. Rosenkrantz AB, Geppert C, Grimm R, Block TK, Glielmi C, Feng L, et al. Dynamic contrast-enhanced MRI of the prostate with high spatiotemporal resolution using compressed sensing, parallel imaging, and continuous golden-angle radial sampling: preliminary experience. *J Magn Reson Imaging* 2014; **41**: 1365–73. doi: 10.1002/jmri.24661
29. Zhang T, Chowdhury S, Lustig M, Barth RA, Alley MT, Grafendorfer T, et al. Clinical performance of contrast enhanced abdominal pediatric MRI with fast combined parallel imaging compressed sensing reconstruction. *J Magn Reson Imaging* 2014; **40**: 13–25. doi: 10.1002/jmri.24333
30. Persons K, Palisson P, Manduca A, Erickson BJ, Savcenko V. An analytical look at the effects of compression on medical images. *J Digit Imaging* 1997; **10**(3 Suppl 1): 60–6. doi: 10.1007/BF03168659
31. Koff D, Bak P, Brownrigg P, Hosseinzadeh D, Khademi A, Kiss A, et al. Pan-Canadian evaluation of irreversible compression ratios ("lossy" compression) for development of national guidelines. *J Digit Imaging* 2009; **22**: 569–78.
32. Gallas BD, Chan HP, D'Orsi CJ, Dodd LE, Giger ML, Gur D, et al. Evaluating imaging and computer-aided detection and diagnosis devices at the FDA. *Acad Radiol* 2012; **19**: 463–77. doi: 10.1016/j.acra.2011.12.016
33. Greengard L, Lee J-Y, Inati S. The fast sinc transform and image reconstruction from non-uniform samples in k-space. *Comm Appl Math Comp Sci* 2006; **1**: 121–32.
34. Lustig M, Pauly JM. SPIRiT: iterative self-consistent parallel imaging reconstruction from arbitrary k-space. *Magn Reson Med* 2010; **64**: 457–71. doi: 10.1002/mrm.22428
35. Feng L, Srichai MB, Lim RP, Harrison A, King W, Adluru G, et al. Highly accelerated real-time cardiac cine MRI using k–t SPARSE-SENSE. *Magn Reson Med* 2013; **70**: 64–74. doi: 10.1002/mrm.24440
36. Uecker M, Lai P, Murphy MJ, Virtue P, Elad M, Pauly JM, et al. ESPIRiT—an eigenvalue approach to autocalibrating parallel MRI: where SENSE meets GRAPPA. *Magn Reson Med* 2014; **71**: 990–1001.
37. Zhang T, Pauly JM, Levesque IR. Accelerating parameter mapping with a locally low rank constraint. *Magn Reson Med* 2015; **73**: 655–61. doi: 10.1002/mrm.25161
38. Antonini M, Barlaud M, Mathieu P, Daubechies I. Image coding using wavelet transform. *IEEE Trans Image Process* 1992; **1**: 205–20. doi: 10.1109/83.136597
39. Miao J, Huang F, Narayan S, Wilson DL. A new perceptual difference model for diagnostically relevant quantitative image quality evaluation: a preliminary study. *Magn Reson Imaging* 2013; **31**: 596–603.
40. Chan KK, Lou SL, Huang HK. Full-frame transform compression of CT and MR images. *Radiology* 1989; **171**: 847–51. doi: 10.1148/radiology.171.3.2717763
41. Terae S, Miyasaka K, Kudoh K, Nambu T, Shimizu T, Kaneko K, et al. Wavelet compression on detection of brain lesions with magnetic resonance imaging. *J Digit Imaging* 2000; **13**: 178–90. doi: 10.1007/BF03168393
42. Macovski A. Noise in MRI. *Magn Reson Med* 1996; **36**: 494–7.
43. Sodickson DK, Hardy CJ, Zhu Y, Giaquinto RO, Gross P, Kenwood G, et al. Rapid volumetric MRI using parallel imaging with order-of-magnitude accelerations and a 32-element RF coil array: feasibility and implications. *Acad Radiol* 2005; **12**: 626–35. doi: 10.1016/j.acra.2005.01.012
44. Lin F-H, Kwong KK, Belliveau JW, Wald LL. Parallel imaging reconstruction using automatic regularization. *Magn Reson Med* 2004; **51**: 559–67. doi: 10.1002/mrm.10718
45. Sánchez-González J, Tsao J, Dydak U, Desco M, Boesiger P, Paul Pruessmann K. Minimum-norm reconstruction for sensitivity-encoded magnetic resonance spectroscopic imaging. *Magn Reson Med* 2006; **55**: 287–95. doi: 10.1002/mrm.20758
46. Graff CG. Framework for task-based assessment of MR image quality. *Proc Intl Soc Mag Reson Med* 2013; **21**: 701.